

## Influence of nano-structural feature of $M_{0.25}Ce_{0.75}O_{1.875}$ (M=Gd, Yb, Y) solid electrolytes on their electronic properties

Toshiyuki MORI,\* Richard BUCHANAN,\* Ding Rong OU,\* Fei YE,\* Hirokazu SUGA\*\*\*\*  
and John DRENNAN\*\*

\*Fuel Cell Materials Center, National Institute for Materials Science, 1-1 Namiki, Tsukuba, Ibaraki 305-0044, Japan  
E-mail: MORI.Toshiyuki@nims.go.jp

\*\*Centre for Microscopy and Microanalysis, The University of Queensland, St. Lucia, Brisbane, 4072 Queensland, Australia

\*\*\*Faculty of Engineering, Saitama University, Shimo-okubo 255, Sakura-ku, Saitama city, Saitama 338-8570, Japan

For a design of ideal structure in doped  $CeO_2$  solid electrolytes, micro-structures of  $M_{0.25}Ce_{0.75}O_{1.875}$  (M=Gd, Yb, Y) sintered bodies were characterized using Transmission Electron Microscopy. This micro-analysis indicates that micro-domain with ordered structure of oxygen vacancy is present in the sintered bodies. It is concluded that the micro-domain consists of a transition structure between fluorite and superstructure such as C-type rare earth structure. On the microanalysis data, we proposed our original idea of conduction mechanism in nano-hetero structured doped  $CeO_2$  solid electrolytes. In our idea, the space charge layer exists around micro-domains. This nano-structural feature is subtle, but it is concluded that the oxide ionic conductivity is conspicuously influenced by this subtle change in the grain.

**Key words:** Nano-structure, doped  $CeO_2$  electrolyte, micro-domain, micro-analysis, fuel cell application

### 1. Introduction

Doped ceria ( $CeO_2$ ) compounds are fluorite type oxides, which show oxide ionic conductivity higher than yttria stabilized zirconia (YSZ), in oxidizing atmospheres. YSZ and scandia stabilized zirconia (SSZ) are common electrolytes used in solid oxide fuel cells (SOFCs).[1,2] However, their respective ionic conductivities do not allow for 'intermediate temperature' (300 - 500°C) operation of SOFCs. Accordingly, it is important that a high-quality electrolyte materials with higher oxide ion conductivity than that of YSZ and SSZ be identified – the systems based on  $CeO_2$  fit this demand. As a consequence, considerable interest has been shown in application of these materials for 'intermediate temperature' (300 - 500°C) operation of SOFCs. In the present study, some kinds of rare earth (i.e. Gd, Yb, or Y) doped  $CeO_2$  nano-powders were synthesized via a carbonate co-precipitation method at elevated temperature such as 75°C. Fluorite-type solid solution was able to be formed at low temperature, such as 400°C and dense sintered bodies were subsequently fabricated in the temperature ranging from 1000° to 1450°C by conventional sintering (CS) method. To develop high quality doped  $CeO_2$  solid electrolytes, the microstructure at the atomic level of these doped  $CeO_2$  solid electrolytes were examined using transmission electron microscopy (TEM). The specimens obtained by CS had continuous and large micro-domains with a superstructure within each grain. We conclude that the conducting properties in these doped  $CeO_2$  systems are strongly influenced by the micro-domain size in the grain.[3-5] To conclude the formation

mechanism of the micro-domain, influence of intensity of extra reflections and diffuse scattering in the selected area electron diffraction patterns on sintering temperature was examined. The observed electron diffraction pattern clearly indicates that micro-domains were developed in the sintering process at high temperature (such as 1400°C or more). This suggests us that careful control of doped  $CeO_2$  particles characters (i.e. particle size, particle morphology) and sintering temperature is required for the successful design of electrolyte materials with improved conductivity.

### 2. Experimental

**Powder synthesis and sintered body fabrication**– The starting materials used for Gd doped  $CeO_2$ , Yb doped  $CeO_2$ , and Y doped  $CeO_2$  synthesis were cerium nitrate hexahydrate ( $Ce(NO_3)_3 \cdot 6H_2O$ ; >99.99% pure, KANTO Chemical Co. Inc., Japan), gadolinium nitrate hexahydrate ( $Gd(NO_3)_3 \cdot 6H_2O$ ; >99.95% pure, KANTO Chemical Co. Inc., Japan), ytterbium nitrate hexahydrate ( $Yb(NO_3)_3 \cdot 6H_2O$ ; >99.95% pure, KANTO Chemical Co. Inc., Japan), yttrium nitrate hexahydrate ( $Y(NO_3)_3 \cdot 6H_2O$ ; >99.95% pure, KANTO Chemical Co. Inc., Japan) and ammonium carbonate ( $(NH_4)_2CO_3$  (Ultrahigh purity, Kanto chemical Co. Inc., Japan). The cerium nitrate hexahydrate and the relevant dopant nitrate hexahydrate powders were dissolved in distilled water, and the solutions were mixed in order to prepare the fixed composition of  $M_{0.25}Ce_{0.75}O_{1.875}$  (M: Gd, Yb, or Y). An aqueous solution of ammonium carbonate in distilled water with a concentration of 1.5M was used as the precipitant. The mixed solutions

were added into the ammonium carbonate solution kept at 75°C whilst being gently stirred. After repeated washing, the precipitate was dried at room temperature in a nitrogen gas flow and then calcined in flowing oxygen at 550 - 800°C for 2h to yield the rare-earth doped powders. These powders were initially molded at a pressure of 98MPa and then subjected to a further pressing using a rubber die at 390MPa in order to obtain a green body. CS temperature ranged from 1000° to 1550°C for 6 hrs.

**Sample characterization** - The crystal phases in the powder and sintered specimens were investigated using X-ray diffraction analysis (XRD, monochromated Cu K $\alpha$ , 50KV, 25mA) and a selected area electron diffraction analysis, respectively. Simulated electron diffraction pattern was calculated using software *CaRIne* (CaRine Crystallography, version 3.1 (presented by Boudias and Monceau (CaRine Crystallography, Senlis, France)). The bulk density of the sintered body was measured using the Archimedes method. The relative density was calculated from the ratio of the measured bulk density to the theoretical density. The theoretical density was estimated using the lattice constant and the sample composition. The particle sizes in the synthesized powders and the grain sizes in the sintered bodies were observed using scanning electron microscopy (SEM). The average grain size in the sintered body was calculated using the linear intercept method, measuring more than 300 grains recorded using micrographs produced by a SEM.[6] The microstructural features in the grain were investigated in detail using TEM. Ion beam thinned specimens were used for TEM observation. In order to avoid reduction of CeO<sub>2</sub> by ion beam milling, Ar ion beam was irradiated using cooled cold stage in liquid nitrogen. TEM observation was performed with gun voltages of 200keV.

**Measurement of electrical properties** - Electrical conductivity of the sintered specimens was measured by dc three-point measurements at 400° - 650°C in air. A platinum electrode was applied to both sides of the sintered bodies at 1000°C for 1h in air. The dimensions of the specimens were 10mm in diameter and 2mm in thickness for the three-point measurements. The activation energy was calculated using the data of conductivity at the temperature ranging from 400° to 650°C.

### 3. Results and discussion

Crystallization of powder occurred above 300°C. The calcined powders consisted of simple fluorite structure, and no other phases were observed in XRD patterns as shown in our previously reported data.[3-5] The powders showed that improved crystallinity developed at temperatures over 400°C. As a consequence all subsequent calcinations were carried out at temperatures between 300° to 800°C. The morphology of dried particles and calcined particles are shown in **Figure 1 (a) and (b)**

respectively. The dried CeO<sub>2</sub> particles doped with Gd<sup>3+</sup> showed no appreciable morphologic changes as a result of calcination. Both dried and calcined powders were observed to be composed of uniformly sized, round, and discrete particles. The average particle sizes of both powders were in the range of between 20 and 30nm.

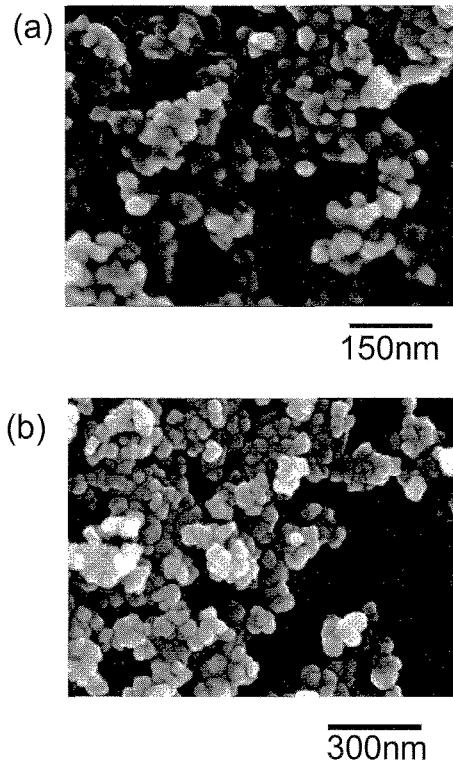
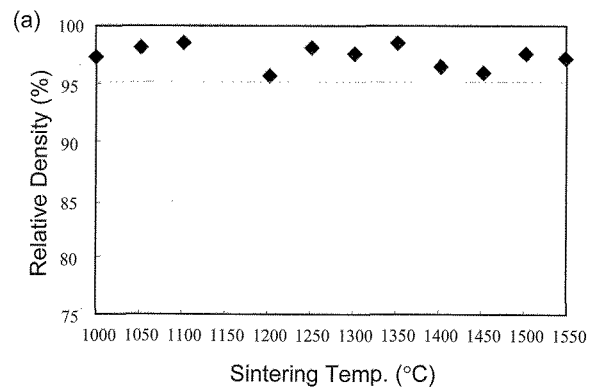


Figure 1 SEM photographs of dried and calcined powders of  $Gd_{0.25}Ce_{0.75}O_{1.875}$ , Calcination temperature: 800°C

**Figure 2** shows sintering temperature dependence of relative density (a) and sintering temperature dependence of average grain size (b) of  $Gd_{0.25}Ce_{0.75}O_{1.875}$ , respectively. This powder can be sintered to over 95% dense of theoretical density (7.243 g/cm<sup>3</sup>) in the temperature range of 1000° to 1550°C using CS method as shown in Fig.2(a).

The average grain sizes were in the range of 0.25 to 3.1 $\mu$ m.



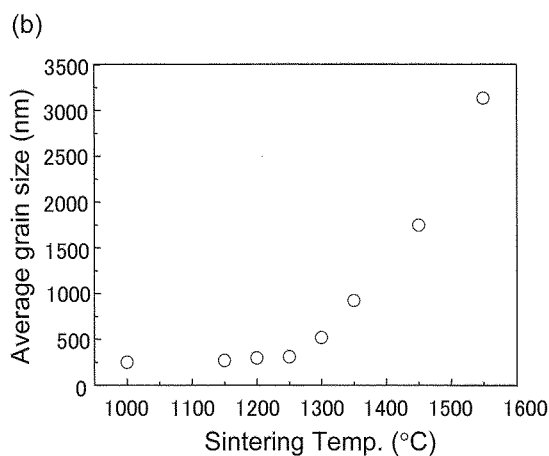


Figure 2 Sintering temperature dependences of relative density (a) and average grain size (b) of  $Gd_{0.25}Ce_{0.75}O_{1.875}$ .

From these figures (i.e. Fig.2(a) and (b)), the grain size appeared to increase exponentially with sintering temperature in the temperature region from 1250 to 1550°C, as observed in Fig.2b. This curve implies that a diffusion-related process in the grain of sintered bodies is activated in the temperature ranging from 1250 to 1550°C. The micro-structural features at atomic scale would be influenced by this diffusion process in the dense sintered bodies.

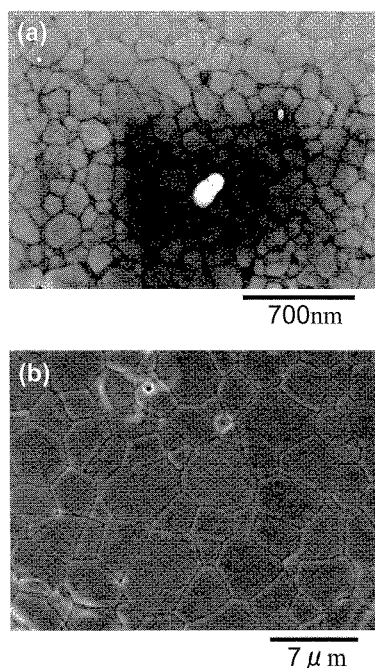


Figure 3 SEM photographs recorded from  $Gd_{0.25}Ce_{0.75}O_{1.875}$  specimens sintered at (a) 1000°C and (b) 1550°C.

SEM photographs of microstructure of CS specimens are shown in Figure 3 (a) and (b). These photographs clearly show that all specimens are dense and few pores were observed in the microstructure. The grain size of specimens sintered at 1550°C was 1 to 7µm, this is in

contrast to the specimen with an average grain size 180nm to 330nm which was sintered to high density at 1000°C. It is concluded that the specimens in Fig.3 provide us a unique opportunity to know the differences of the internal microstructures at the atomic level of these materials as a function of sintering temperature.

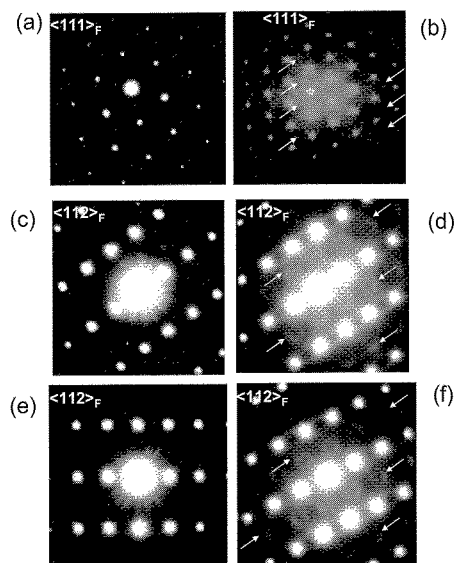


Figure 4 Selected area electron diffraction patterns recorded from (a):  $Gd_{0.25}Ce_{0.75}O_{1.875}$  sintered at 1000°C, (b):  $Gd_{0.25}Ce_{0.75}O_{1.875}$  sintered at 1450°C, (c):  $Yb_{0.25}Ce_{0.75}O_{1.875}$  sintered at 1000°C, (d):  $Yb_{0.25}Ce_{0.75}O_{1.875}$  sintered at 1450°C, (e):  $Y_{0.25}Ce_{0.75}O_{1.875}$  sintered at 950°C, (f):  $Y_{0.25}Ce_{0.75}O_{1.875}$  sintered at 1400°C. Sintering time: 6h, white arrows indicate extra reflections.

Figures 4(a) – 4(f) display the selected area electron diffraction patterns which are recorded from  $M_{0.25}Ce_{0.75}O_{1.875}$  sintered bodies. The diffuse scattering clearly exists in the background of electron diffraction patterns in Figs 4(b), (d), and (f). This indicates that micro-domain with coherent interface is present in the grain of specimens which are sintered at 1400°C or 1450°C. In addition, very small extra spots which are indicated by white dashed arrow lines coexisted with main fluorite type spots in the same electron diffraction patterns. These extra spots indicate that micro-domain consists of super-structure (Figs 4(b), 4(d), and 4(f)). On the other hand, the extra reflection and diffuse scattering are very small in Figs 4(a), 4(c), and 4(e). This suggests that micro-domain size is small in the specimens sintered at low temperature (<1000°C).

Usually, the lower valence cation such as Gd, Yb or Y was dissolved into tetra valence Ce site to create the oxygen vacancy. However, small amount of dopant cation would be segregated around grain boundary. The lattice distortion would be introduced into fluorite lattice by this

segregation. To minimize the lattice distortion in  $CeO_2$  lattice, micro-domain with ordered structure would be formed in the lattice. The micro-domain would be developed in the grain to minimize this lattice distortion. The influence of sintering temperature on growth of micro-domain within grain was illustrated in Fig.5.

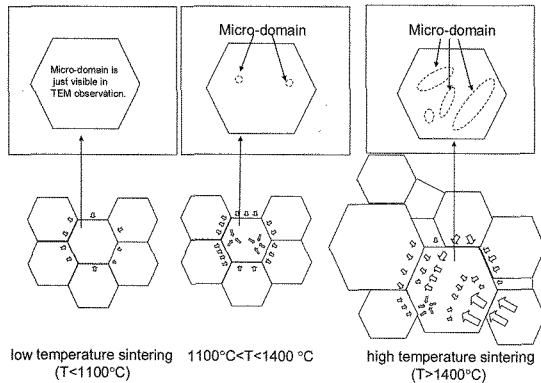


Figure 5 Relationship between sintering temperature and micro-domain size in the grain of  $M_{0.25}Ce_{0.75}O_{1.875}$  ( $M: Gd, Yb, \text{ or } Y$ ) sintered bodies.

The specimen sintered below  $1100^\circ C$  consists of homogeneous grain size. In this specimen, lattice distortion would be small. Then micro-domain size is just visible in TEM analysis. Since the lattice distortion in the specimen sintered above  $1400^\circ C$ , the size of micro-domain was over 20 nm in the sintered body. Some micro-domains combined with each other and became the continuous micro-domain with irregular shapes. It is concluded that the oxide ionic conductivity is influenced by the micro-domain size.

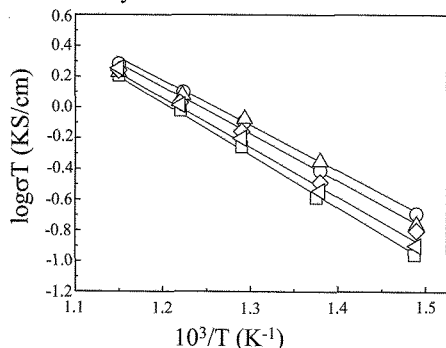


Figure 6a Temperature dependence of DC conductivity in  $Gd_{0.25}Ce_{0.75}O_{1.875}$   $\Delta$ : 295nm,  $\circ$ : 310nm,  $\square$ : 520nm,  $\diamond$ : 1750nm,

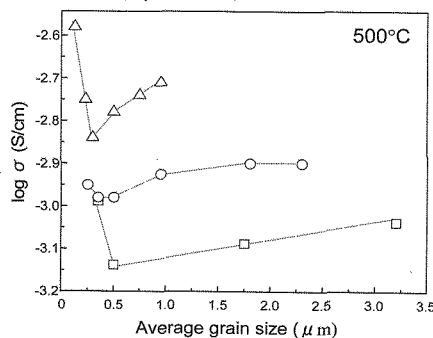


Figure 6b Average grain size dependence of conductivity in  $M_{0.25}Ce_{0.75}O_{1.875}$  ( $M: Gd (\square), Yb (\circ), Y (\Delta)$ ).

Figure 6a presents the temperature dependence of conductivity in Gd doped  $CeO_2$  specimens with different average grain size. The activation energy of these specimens was from 55 to 62kJ/mol. These values almost agree with previously reported data.[7] In addition, the other specimens have similar tendency compared with Gd doped  $CeO_2$  specimens. The conductivity in the three kinds of specimens showed the curvature in the grain size dependence of conductivity, as shown in Fig. 6b. The conductivity decreased with decreasing grain size and reached the lowest value at similar average grain size (i.e. 250nm to 500nm). This tendency would be attributable to the space charge layer around the grain boundary in the sintered body. On the other hand, the conductivity increased with a decrease of grain size under aforementioned grain size region. In this region, it is suggested that the space charge layer with high resistivity is minimized around the grain boundary. Since the change of conductivity is clear in the small grain size region, other micro-structural features within the grain are also beginning to have an influence. This conclusion agrees with the conclusion in Fig.5. This indicates that the conductivity in doped  $CeO_2$  is influenced by the growth of micro-domain with ordering of oxygen vacancy. In order to maximize the oxide ionic conductivity in doped  $CeO_2$ , the micro-domain size should be minimized by a fabrication of homogeneous microstructure.

#### Summary

The relationship between micro-structural features and conducting property in  $M_{0.25}Ce_{0.75}O_{1.875}$  ( $M: Gd, Yb, \text{ or } Y$ ) sintered bodies was examined. The specimens sintered at high temperature (above  $1400^\circ C$ ) had big micro-domains with superstructure. The conductivity in the specimens was influenced by a size of micro-domain. To maximize the conductivity in the specimen, the micro-domain size should be minimized. Accordingly, it is concluded that the design of nano-domain structure is very important for improvement of conducting property in doped  $CeO_2$  solid electrolytes.

#### References

- [1] N.Q.Minh, *J.Am.Ceram.Soc.*, **76**, 563-588 (1993).
- [2] S.M.Haile, *Acta Materialia*, **51**, 5981-6000 (2003).
- [3] T.Mori, J.Drennan, J.-H.Lee, J.-G.Li, and T.Ikegami, *Solid State Ionics*, 154-155, 461-466(2002).
- [4] T.Mori, J.Drennan, Y.Wang, J.-H.Lee, J.-G.Li, and T.Ikegami, *J.Electrochem.Soc.*, **15**(6), A665-A673(2003).
- [5] T.Mori, J.Drennan, Y.Wang, G.Auchterlonie, J.-G.Li, and A.Yago, *J. Science and Technology for Advanced Materials*, **4**, 213-220(2003).
- [6] M.I.Mendelson, *J.Am.Ceram.Soc.*, **52**(8), 443-446 (1969).
- [7] M.Mogensen, N.M.Sammes, G.A.Tompsett, *Solid State Ionics*, **129**, 63-94(2000).

(Received January 5, 2007; Accepted September 1, 2007)